Anticancer Potential of Synthesized Silver Nanoparticles Using Bioactive Metabolites of Actinobacteria Against A549 Lung Cancer Cells

Naushin Bano
Integral University
Saba Siddiqui
Integral University
Adria Hasan
Integral University
Mohammad Amir
Integral University
Snober S Mir
Integral University
Abu Baker
Integral University
Roohi Roohi (roohi0607@gmail.com)
Integral University https://orcid.org/0000-0003-4296-6105

Research Article

Keywords: Actinobacteria, Secondary metabolites, silver Nanoparticles, Anticancer activity, Lung cancer cells, Antibacterial activity

Posted Date: November 12th, 2021

DOI: https://doi.org/10.21203/rs.3.rs-1054044/v1

Abstract

Multi-drug resistance microorganisms and the rising numbers of cancer cases possess a critical threat to humankind, thereby motivating research on new weapons to combat the problem. To address these issues, researchers are now focusing on secondary metabolites produced by bacteria. Because of having outstanding antibiotic capabilities, actinobacteria are being explored as a potential solution to this problem. Silver nanoparticles of actinobacteria are green, eco-friendly, and cost-effective, as well as having antibacterial and anti-cancer properties and potential use in pharmaceuticals. Antibacterial potential of secondary metabolites produced by actinobacteria namely *Microbacterium proteolyticum* LA2(R) and *Streptomyces rochei* LA2(O) has been demonstrated by the well diffusion method. GC-MS was used to detect compounds in bioactive metabolites. The most abundant compound found in metabolites was n-hexadecanoic acid. UV-Vis spectroscopy was used to determine the extracellular development of silver nanoparticles of actinobacteria secondary metabolites, while transmission electron microscopy (TEM) and Fourier transform infrared spectroscopy (FTIR) were used to inspect their morphological appearances, stability, crystalline structure, and coating. The activity of anticancer was assessed using the MTT test to evaluate the cytotoxicity of the secondar metabolites (pure and nanoparticles) against A549 lung cancer cells. We also evaluated the effect of secondar metabolites (pure and nanoparticles) on Reactive oxygen species (ROS) levels, Mitochondrial membrane potential (MMP) and Chromatin condensation through DCFDA, Mito Tracker and DAPI staining. Our result suggested that their secondary metabolites can be used a potential lead compound against cancer. However, more investigation is needed to totally grasp their mechanism of action.

Introduction

Approximately 10 million deaths occur each year as a result of cancer, which is the subsequent biggest reason of mortality in the globe. According to the WHO report, the principal cause of cancer death in 2020 was Lung cancer (WHO, 2020). The resistance of chemotherapeutic drugs is arising in cancer cells, so lung cancer needs various therapy lines for treatment. Despite advances in elucidating the molecular processes behind lung cancer and collaboration in the development of screening strategies for the prevention of secondary cancers, the diagnosis of the patient remains poor and making lung cancer a global killer (de Groot et al. 2018; Hasan et al. 2020). Nanotechnology proposes assets of tools to analyze and treat various cancers with the minimum costs and side effects (Bano et al. 2019; Iram et al. 2019). Green nanoparticle synthesis is clean, nontoxic and safe, low-cost, and ecologically friendly. Amongst the variety of accessible biological processes, microbial synthesis is mostly impractical, as they require a sterile environment (Al-Sheddi et al. 2018). Nanoparticles of silver have gained a great deal of attention in the field of metal nanomaterials because of their physico-chemical properties. Antimicrobial activities and therapies, bimolecular recognition, biolabeling, catalysis and microelectronics, etc., are just a few of the uses (Abd-Elnaby et al. 2016). According to studies, actinobacteria-produced nanoparticles offer a wide range of applications in nanomedicine to battle new microbial pathogens (Sivasankar et al. 2019). Actinobacteria provide good prospects for the manufacture of metal nanoparticles both

extracellularly and intracellularly. The actinobacteria have developed good stability and polydispersity in their synthesis of nanoparticles (Abd-Elnaby et al. 2016).

Novel antibiotics and anticancer medicines with unique structures and properties have recently been discovered as the product of research on actinobacteria (Manivasagan et al. 2014; Ravikumar et al. 2012). While these cancer-fighting medications may have secondary effects such as requiring higher doses, and weaker blood flow for osteosarcoma patients, a patient's genetic profile can influence drug use outcomes. Recently, synthesized nanoparticles have emerged as a critical tool in cancer treatment. In addition to decreasing side effects, they have the ability to improve pharmaceutical delivery or absorption, or reduce toxicity in surrounding tissues. In addition to decreasing side effects, they have the ability to improve pharmaceutical delivery or absorption, or reduce toxicity in surrounding tissues. Some of the biological synthesis methods for nanoparticles provide considerable advantages, like being inexpensive, easy, and creating nanoparticles under a physiologically safe pH and room temperature.

Materials And Method

Isolation of actinobacteria

A total of five soil samples have been obtained from rhizosphere of medicinal plants i.e., *Asparagus racemosus*, *Withania somnifera, Salvia officinalis, Rouwolfia serprntina,* and *Ocimum sanctum* from different locations of Lucknow, Uttar Pradesh, and kept in sterilized plastic bags at 4ºC (Lee et al. 2014). Eleven actinobacterial isolates representing different colony morphologies were isolated and cultivated on actinomycetes isolation agar for five to seven days at ±28℃ (Sharma and Thakur 2020).

Preliminary Antimicrobial screening of Actinobacteria

Primary screening was done by single streak of positive isolate of actinobacteria against pathogenic and Multi drug resistant (MDR) microbes streak at 90° on Mueller Hinton agar (Elbendary et al. 2018). The actinobacterial isolates were streaked as a parallel line on Mueller Hinton agar for bacteria and potato dextrose agar plates for fungi and incubated at 28˚C for 4-6 days (Ganesan et al. 2017). When actinobacterial strains properly grown on media, selected pathogenic bacterial strains i.e., *Staphylococcus aureus* (ATCC-6538), *Pseudomonas aeruginosa* (NCIM-5029)*, Salmonella abony* (ATCC-6017), *Klebsiella pneumoniae* (NCIM-2957)*, Bacillus subtilis* (MTCC-441) and *Escherichia coli* (MDR) (ATCC-25923) and pathogenic fungi i.e., *Aspergillus niger* (ITCC 545)*, Aspergillus flavus* (MTCC277)*, Aspergillus parasiticus* (MTCC-2796) were streaked at right angles to the previous streak of actinobacteria and incubated at 30˚C. The A measurement of the zone of inhibition was taken after 72 hours for fungi and 24 hours for bacteria. Seven actinobacterial isolates were found positive after primary screening and subjected to molecular characterization.

Molecular characterization of positive isolates

The selected isolates from the secondary screening were subjected to molecular characterization using 16S rRNA sequence amplification performed at Bio-kart India Pvt. Ltd, Bangalore. The 16S ribosomal sequence amplification was conducted using the primers F243 (5'GGATGAGCCCGCGGCCTA3') and 1378R (5'CGGTGTGTACAAGGCCCGG 3'). Subsequently, the construction of phylogenetic tree by MEGA6 software, by applying the neighbor-joining DNA distance algorithm. The results of the microbial characterization revealed two isolates, i.e., LA2(R) *Microbacterium Proteolyticum* (MN560041) and LA2(O) *Streptomycetes rochei* (Zothanpuia 2015; Ganesan et al. 2017).

Production of secondary metabolites

The primarily screened actinobacteria with antimicrobial activities were used for the extraction of secondary metabolite. Production of secondary metabolites from actinobacteria was done by submerged state fermentation (SmF) (Salim et al. 2017). The isolates LA2(R) *Microbacterium Proteolyticum* and LA2(O) *Streptomycetes rochei* were inoculated in 500 ml flask containing 100 ml of ISP-2 medium (g/L): yeast extract, 4.0; malt extract, 10.0; dextrose, 4.0; Agar, 20.0; distilled water, 1000 mL and pH 7.3. The flasks with inoculated strains were incubated for 5-7 days at 200 rpm in rotary shaker. The cultures was centrifuged at 10,000 rpm after the growth, and its supernatant was used for future experimentations (Abd-Elnaby et al. 2016; Singh and Dubey 2020).

Green synthesis of silver nanoparticle

Silver nanoparticles *in-vitro* production, was carried out by using the 1 mM aqueous solution of 50 µl $AgNO_3$, that was pre-mixed with 50 ml supernatants of actinobacteria at 8.5 pH (Abd-Elnaby et al. 2016). In rotary shaker at 200 rpm, and suspension was incubated in the dark at 37°C. for 5 days. To evaluate whether bacteria are involved in nanoparticle creation, the control tests involved running the process using un-inoculated medium and $AgNO_3$ solution. Silver ions reduction was tested by taking samples at specified intervals, using a UV–Vis spectrophotometer, and monitoring the UV–Vis spectrum. The color of silver nitrate solution changed to yellowish brown in each reaction vessel, which was then incubated with actinobacteria supernatant (Azman et al. 2017; Al-Sheddi et al. 2018).

Characterization of synthesized silver nanoparticle

To demonstrate the formation of extracellular silver nanoparticles, UV–visible spectroscopy and transmission electron microscopy were used to examine synthesized AgNPs. The preliminary synthesis of AgNPs was authenticated using a UV–visible spectrophotometer (Shimadzu dual beam-model UV-1601 PC) with a wavelength of 1 nm. A drop of AgNps (suspension) was dried on a carbon-coated TEM copper grid at a step-up voltage of 80 kV with a TEM Tecnai^{TM} G2 Spirit Bio-TWIN (FEI, Hillsboro, OR, USA) to assess the proportions of the inorganic core.

FT-IR spectroscopy of biogenic AgNPs

Existence of diverse functional groups was inveterate by Perkin-Elmer Spectrum 2 FT-IR (PerkinElmer Inc., Waltham, MA, USA), at the surface of AgNps. In this method, samples are held by a worldwide attenuated complete reflectance sampling instrument, which is diminished with respect to the entire surface, and is scanned through a transmission technique with a resolution of 4 cm^{-1} above the wave number range of 4,000–4500 cm^{-1}. The FTIR aim is to measure how much light, at each wavelength, absorbed by the samples (Barapatre et al. 2016).

Anticancer studies

Adenocarcinoma cells from the National Centre for Cell Science (NCCS) in Pune, India, were obtained and Incubated at 37°C with 5 percent Carbon dioxide in Dulbecco's Modified Eagle Medium/Nutrient Mixture F-12 Ham (DMEM/F12, HiMedia-AT155) medium supplemented with 10 percent foetal bovine serum (FBS, HiMedia-RM10432) and 1percent of antibiotic or antimycotic solution (HiMedia-A002) (Ravikumar et al. 2012).

MTT assay

To check the feasibility of cells, an MTT (3-(4, 5-Dimethylthiazol-2-yl)-2, 5-diphenyltetrazolium bromide) assay was accomplished. It is a colorimetric assay used to determine the activity of cellular enzymes responsible for reduction of the tetrazolium dye MTT to formazan crystals, which results in a purple color. $1x10^4$ cells/well were seeded in 96-well plate and were cultivated to about 70% confluency. Different concentrations of chemicals were used to treat the cells, secondary metabolite of LA2(R) and LA2(O) and their silver synthesized nanoparticles LA2(RN) and LA2(ON) and 5-FU for 24 hours. Further MTT was performed as described earlier by Hasan et. al. (Hasan et al. 2020).

ROS determination cell line of lung cancer

A solution of 2,7-dichlorofluorescein diacetate was used to measure the level of intracellular ROS production (carboxy-DCFDA, Molecular Probes-D369, Invitrogen). In a 24-well plate, cells were plated and treated with compounds (LA2(R), LA2(O), LA2(RN), LA2(ON) and 5-FU) for 24 hours. Image J software was used to evaluate the fluorescence strength of stained cells (Hasan et al. 2020).

DAPI staining to verify the impact of compounds on DNA integrity

4, 6-diamidine-2-phenylindole (DAPI), Molecular Probes-D1306, Invitrogen, staining was done as stated by the manufacturer. Briefly, the cells were cultured and treated with LA2(R), LA2(O), LA2(RN), LA2(ON) and 5-FU, in a 24-well plate, for 24 h. Image J software was used to evaluate fluorescence strength of stained cells (Hasan et al. 2020).

MMP staining

MMP staining (Mito Tracker Red) was used for the determination of the influence of compounds on membrane potential of mitochondria. After 24-hour exposure to compounds (LA2(R), LA2(O), LA2(RN),

LA2(ON) and 5-FU). Cells (treated and untreated both) became stained after being washed twice in PBS for 30 minutes with 300 nM Mito Tracker Red CMXRos fluorescent dye (Molecular Probes-M7512, Invitrogen) at room temperature in the dark (Hasan et al. 2020). Fluorescent images after washing in PBS were obtained using a Thermo-Scientific EvosFLc Microscope at an excitation wavelength of 579 nm and an emission wavelength of 599 nm. By using the Image J software, we were able to determine the fluorescence intensity of the stained cells (Abd-Elnaby et al. 2016).

Statistical evaluation

One-way ANOVA was performed using Graph Pad prism 5 for statistical analysis on the data. The results were provided as the mean standard deviation of at least three independent measurements (nonsignificant (ns), *p 0.05, ** p 0.01, *** p 0.001 against the untreated control).

Results

Isolation of actinobacteria

Five rhizospheric soil samples of medicinal plants were air-dried and pretreated with $CaCO_3$ and then serial dilution was carried up to 10^{-5} factors, spread on specific agar and pure colonies were isolated by streak plate technique. After streaking, eleven pure isolates were found initially according to the morphological appearance of the colonies. The isolated isolates were filamentous, Gram-positive, non-motile, and aerobic, with Catalase and Oxidase activity.

Preliminary screening and metabolite production

During preliminary screening, all 11 actinobacteria were tested for their ability to produce antimicrobials against pathogenic microorganisms. With the help of the perpendicular streak method, actinobacteria are tested for antimicrobial activity and seven strains are found positive.

Molecular characterization of positive isolates

All seven pure and active microbial strain cultures chosen during the primary screening experiments are further subjected for molecular characterization and found confirmation of two positive isolates named LA2(O) and LA2(R) using 16S rRNA sequence amplification. Further, the phylogenetic analysis confirmed that the isolates are *Microbacterium proteolyticum* LA2(R) and *Streptomyces rochei* LA2(O). The phylogenetic tree of the isolate *Streptomyces rochei* LA2(O) is characterized in Fig 1(a). The partial 16S rRNA gene sequence of isolate LA2(R) has been submitted in the NCBI GenBank with the accession number MN560041. Phylogenetic tree of the isolate LA2(R) is depicted in Fig. 1(b).

Production of secondary metabolites

After fermentation of ISP-2 broth, supernatant is extracted using ethyl acetate. After liquid-liquid extraction, the solvent phase is separated and crude extract was obtained after evaporation of solvent

with the help of rotatory vacuum evaporator and mixed with methanol and stored for further use (fig. 2). The metabolite production by submerged state fermentation techniques shows good results of antimicrobial activity against *Staphylococcus aureus* (ATCC-6538) and *Klebsiella pneumoniae* (NCIM-2957) as shown in Fig. 3.

Gas chromatography–mass spectrometry

The metabolite extract of LA2(R) and LA2(O) was subjected to GC-MS analysis. Identification of the compounds was based on the peak area, molecular weight and formula and similarity index. The GC-MS analysis of ethyl acetate extract of *Streptomycetes rochei* LA2(O) and *Microbacterium proteolyticum* LA2(R) are shown in Fig. 4 (a) and 4 (b), respectively. The compounds result shown by GC-MS analysis are presented in the Table 1. n-Hexadecanoic acid was the major compound present in both extracts with 95% and 92 % similarity index, respectively.

Synthesis of silver nanoparticle

The AgNPs were synthesized by incubating 1 mM AgNO3 with 333 µg/ml of secondary metabolites LA2(R) and LA2(O) at 40°C for 48 hours. It is proposed that Secondary metabolites, which together possess a synergistic ability to generate reducing potential capable of neutralizing AgNO3 (aq) into Ag (aq) NPs in aqueous solution. The efficacy of the presence of a response in the absence of salt has been verified. Secondary metabolites in the synthesis of AgNps. Similarly, incubation of secondary metabolites alone in distilled water did not result in the formation of any AgNPs specific assimilation peak(s). The characteristic absorption maximum centered at 422 nm (Fig. 5A) for strain LA2(R) (RAgNPs) and 419 nm (Fig. 5B) for strain LA2(O) (OAgNPs) accredited to the surface plasmon resonance (SPR) band of the AgNPs. TEM analysis of the samples was measured by the average size of RAgNPs to be 23±2 nm (Fig. 5C) and OAgNPs to be 20±2 nm (Fig. 5D). Additional inspection of the TEM micrograph using the Gatan Digital Micrograph revealed that the NPs were spherical in shape. The TEM micrographs revealed discrete, well-separated AgNPs particles.

FTIR (Fourier transform infrared spectral) study of RAgNPs and OAgNPs (Fig. 5E, 5F) existing peaks positioned at 1,639.92 cm^{-1} and 1637.69 cm^{-1} appearances of C=O of amide groups of the amide I linkage. The amide bands are caused by carboxyl stretch and N-H deformation vibrations in the amide bonds of the proteins that contained the AgNps. In addition, peak at 3405.88 cm^{-1} and 3416.74 cm^{-1} confirms the N-H stretching vibration. This mode of vibration is insensitive to the strength of a hydrogen bond and is not dependent on the backbone conformation. Moreover, a peak at 711.03 cm^{-1} and 1065.35 cm^{-1} shows (C-O-C/C-OH) C-O stretching of alcohol and ether group with C-N (aliphatic amine) stretching vibration. Due to the presence of various secondary metabolites, a peak at 2086.14 cm^{-1} and 2094.22 cm^{-1} represents C≡C stretch of alkynes. Terminal-free hydroxyl (O-H) is represented by representative peaks 3405.88 cm^{-1} and 3416.74 cm^{-1}.

Anticancer studies of Actinobacteria

MTT assay of the secondary metabolites and their respective silver nanoparticles

The MTT assay was used to determine cytotoxicity of compounds (LA2(O), LA2(R), LA2(ON), and LA2(RN)) against a cell line of human lung cancer A549. The secondary metabolites (LA2(O), LA2(R)), and their silver nanoparticles (LA2(ON), LA2(RN)) cytotoxic activity was compared to that of 5-FU. In this investigation, 5-FU, a notable anticancer medication, was employed as a positive control. It acts by preventing the synthesis of thymidine, resulting in cell death. Our results indicate that the compounds significantly decreased A549 cell viability in under 24 hours. The results prove that the compounds. The IC_{50} for 5-FU(a), LA2(O) (b), LA2(R) (c), LA2(ON) (d), and LA2(RN) (e) was obtained at 30 µM (52.73% cell viability), 125 µg (52.35% cell viability), 100 µg (52.3% cell viability), 30 µM (50.25% cell viability), and 70 µM (48.72% cell viability), respectively (Figure 6 a-e).

The secondary metabolites and their respective silver nanoparticles cause oxidative stress on A549 lung cancer cells

Treatment with the compounds caused considerable cell death in A549 cells, according to the findings. The purpose of this study was to investigate whether the cytotoxicity of the compounds is due to the generation of reactive oxygen species. After treating A549 cells with the compounds, ROS levels were measured using DCFDA (2, 7-dichlorodihydrofluorescein diacetate) labelling for 24h (Fig. 7a). Image J software was used to calculate DCFDA staining fluorescence intensity in relation to ROS production (Fig. 7b). The results demonstrated that the compounds compared to untreated, produced higher levels of ROS cells. 5-FU caused 1.97-fold, LA2(O) caused 2.57-fold, LA2(R) caused 2.18-fold, LA2(ON) caused 2.28-fold, and LA2(RN) caused 2.75-fold increase in ROS generation in comparison to untreated A549 lung cancer cells (Fig 7a-b). This data recommended that A549 cells' inhibition of growth in response to chemicals could be attributable to oxidative stress.

The secondary metabolites and their respective silver nanoparticles Reduce MMP to induce apoptosis in A549 cells

An increase in Reactive oxygen species has been referred to mitochondrial damage as well as a reduction in MMP (Cheng et al. 2019) therefore it has been checked that whether the compounds affected Mito Tracker Red staining of mitochondrial content in A549 cells (Fig. 8a). Using Image J software, the fluorescence intensity of Mito Tracker Red staining related to MMP depletion was quantified (Fig. 8b). Our findings revealed that the compounds caused MMP reduction in A549 cells. 5-FU caused 0.35-fold, LA2(O) caused 0.55-fold, LA2(R) caused 0.26-fold, LA2(ON) caused 0.39-fold, and LA2(RN) caused 0.31-fold decrease in MMP in A549 compared to untreated lung cancer cells.

DAPI staining of secondary metabolites and their respective silver nanoparticles

Using DAPI staining, we looked at another characteristic of apoptosis: chromatin condensation. The compounds were introduced to A549 cells for 24 hours and then examined to see if they had any effect on DNA integrity. In comparison to untreated cells, fluorescence pictures of DAPI staining revealed

chromatin condensation in treated cells (Fig. 9a). 5-FU caused 1.49-fold, LA2(O) caused 1.55-fold, LA2(R) caused 1.15-fold, LA2(ON) caused 1.34-fold, and LA2(RN) caused 1.74-fold increase in DAPI fluorescence intensity compared to untreated A549 lung cancer cells (Fig. 9b). Together these results determine that the compounds promote apoptosis in A549 lung cancer cells.

Discussion

The present study showed that the actinobacteria *Microbacterium* sp. LA2(R) and *Streptomycetes* sp. LA2(O) were isolated from less explored rhizospheric soil have potential to produce an array of bioactive metabolites that have promising antibacterial and antifungal potential towards antibiotic-non-resistant and antibiotic-resistant pathogens and tremendous anticancer activity. Singh et. al. (2016) found that fifteen isolates have antibacterial activity against gram positive bacteria and multi drug resistant bacteria by perpendicular streak method (Singh et al. 2016). The metabolite production by submerged state fermentation techniques shows good results of antimicrobial activity (Salim et al. 2017) against pathogenic bacteria. Based on GC-MS analysis, the occurrence of bioactive chemical compounds proved the potential of metabolites. To enhance the potential of these metabolites, the nanoparticle synthesis was formulated by silver nitrate. These AgNPs were fully characterized by UV–Visible spectroscopy, FT-IR and TEM (Baker et al. 2020; Sanjivkumar et al. 2019). Reaction in the absence of salt confirmed the efficacy of secondary metabolites in the synthesis of AgNps (Rivero-Montejo et al. 2021; Musino et al. 2020; Saminathan 2015).

Apoptosis suppression is primary reason of cancer proliferation, and it can be inhibited by a variety of oncogenic routes. The apoptotic route is suppressed in cancer through a number of methods, including anti-apoptotic protein over-expression and pro-apoptotic protein under-expression. Most of these alterations result in innate resistance to chemotherapy, which is the most prevalent anticancer treatment. Finding new compounds that have anticancer potential by stimulating the apoptotic pathway is essential in developing new promising anticancer therapies (Pfeffer and Singh 2018). In this study, we analyzed the anticancer potential of the secondary metabolites derived from *Microbacterium* sp. and S*treptomycetes* sp. on A549 lung cancer cells. Further, silver nanoparticles of the metabolites were made, and their anticancer potential on A549 cells were also assessed. Our results demonstrated that the secondary metabolites (LA2(O), LA2(R)), and their silver nanoparticles (LA2(ON), LA2(RN)) caused cytotoxicity on A549 cells. After exposing A549 cells to the chemicals, an increase in ROS was detected. In cancer cells, ROS buildup plays a key function in apoptosis induction and cell cycle arrest. Numerous chemotherapeutic medications demonstrates their pharmacological properties by generating significant amounts of reactive oxygen species (ROS), which leads to mitochondrial membrane damage and death (Vandamme et al. 2012). Thus, the consequences of the compound on MMP in A549 cells were investigated.

MMP depletion was detected in A549 cells treated with the drugs. At low quantities, ROS is produced inside mitochondria (Santucci et al. 2019) and referred to as a favorable feedback system, entitled “ROS-induced ROS release”(RIRR) continues this interface (Zorov et al. 2000). When mitochondria are

subjected to deleterious events whereas suffering a decrease in transmembrane potential, uncontrolled ROS develops. RIRR causes mitochondrial ROS to be produced, which reduces MMP and causes mitochondrial permeability transition pores to open more slowly (mPTP) (Zorov et al. 2000). Mitochondrial membrane depolarization disrupts mitochondrial respiratory chain activity, this may result in the buildup of reactive oxygen species (ROS) (Fang et al. 2017). Apart from a drop in MMP, another distinct hallmark of apoptosis is membrane blebbing, chromatin condensation, and DNA fragmentation (Chang et al. 1997). Thus, we performed DAPI staining, and upregulation in DNA condensation was observed after treatment with the compounds in A549 lung cancer cells. Overall, our results demonstrated that the compounds were exhibiting early hallmarks of apoptosis. However, further studies are required to thoroughly understand their anticancer potential that may help identify new disease targets, resulting in the development of new treatment techniques for a wide range of disorders. Thus, our findings suggest the anticancer potential of secondary metabolites of actinobacteria and their biosynthesized silver nanoparticles against A549 lung cancer cells that could play an important role in the development of new therapeutic agent for the treatment of cancer.

In short, the current study has showed that these novel and rare actinobacteria were able to produce a wide range of bioactive compounds which could serve as potential sources for future drug development. The present work provides helpful insight into the development of new antimicrobial agents with the synergistic enhancement of the antibacterial mechanism against pathogenic micro-organisms.

Statistical analysis

Statistics were presented as the average of three separate trials' standard deviations. The data analysis was carried out by using Origin 6.0 software, which was developed in the United States, as reported previously (Alvi et al. 2017).

Future perspectives

Green nanoparticle production seems to be in a research phase for cancer treatment and diagnosis, but drug trials are needed to be determined in its final dependability. Due to their biocompatibility and effectiveness, green nanomaterials have opened up plenty of new options in terms of their application. Furthermore, numerous cancers that currently have no solutions may be treated in the future by these green nanomaterials. Given the foregoing, green nanomaterials are predicted to emerge as future cancer treatments and diagnostics compounds in the upcoming future.

Declarations

Funding: This research study was funded by Department of Science and Technology- Science and Engineering Research Board (DST-SERB), Government of India (Project No. ECR/2017/001001) under ECRA scheme.

Conflicts of interest

The authors declare that there are no conflicts of interest.

Authors' contributions

Ms. Bano has conducted all the research experiments and wrote the manuscript in a draft form. Dr. Siddiqui has analyzed the data for microbial experiments. Mr. Amir has made a contribution for statistical analysis in experiments. Ms. Hasan has also given her contribution during conduction of the experiments related to cell lines. Dr. Mir has analyzed the data for Lung cancer cells lines. Mr. Baker has made his contribution for the synthesis of nanoparticles. Dr. Roohi has conceived the idea of this research and designed the protocols for all the experiments.

Data Availability Statement (DAS)

All data generated or analyzed during this study are included in this published article.

Acknowledgement

The authors are grateful to the Department of Science and Technology (DST-FIST) for infrastructural support and Integral University for providing the manuscript communication number IU/R&D/2018-MCN0001194.

References

1. Abd-Elnaby HM, Abo-Elala GM, Abdel-Raouf UM, Hamed MM (2016) Antibacterial and anticancer activity of extracellular synthesized silver nanoparticles from marine *Streptomyces rochei* MHM13. Egypt J Aquat Res 42:301–312
2. Al-Sheddi ES, Farshori NN, Al-Oqail MM, Al-Massarani SM, Saquib Q, Wahab R, Musarrat J, Al-Khedhairy AA, Siddiqui MA (2018) Anticancer potential of green synthesized silver nanoparticles using extract of *nepeta deflersiana* against human cervical cancer cells (HeLA). Bioinorg Chem Appl 2018: 12
3. Alvi SS, Ansari IA, Ahmad MK, Iqbal J, Khan MS (2017) Lycopene amends LPS induced oxidative stress and hypertriglyceridemia via modulating PCSK-9 expression and Apo-CIII mediated lipoprotein lipase activity. Biomed Pharmacother 96:1082–1093
4. Azman AS, Othman I, Fang CM, Chan KG, Goh BH, Lee LH (2017) Antibacterial, Anticancer and Neuroprotective Activities of Rare Actinobacteria from Mangrove Forest Soils. Indian J Microbiol 57:177–187
5. Baker A, Syed A, Alyousef AA, Arshad M, Alqasim A, Khalid M, Khan MS (2020) Sericin-functionalized GNPs potentiate the synergistic effect of levofloxacin and balofloxacin against MDR bacteria. Microb Pathog 148:104467
6. Bano N, Siddiqui S, Amir M, Roohi (2019) House of industrially important bioactive metabolites: A review on actinobacteria. Indian J Biotechnol 18:293–304

7. Barapatre A, Aadil KR, Jha H (2016) Synergistic antibacterial and antibiofilm activity of silver nanoparticles biosynthesized by lignin-degrading fungus. Bioresour Bioprocess 3:1–13
8. Chang GQ, Gaitan A, Hao Y, Wong F (1997) Correlation of DNA fragmentation and chromatin condensation in apoptotic nuclei of the Ser 6 mouse retina. Microsc Res Tech 36:123–129
9. Cheng MH, Huang HL, Lin YY, Tsui KH, Chen PC, Cheng SY, Chong IW, Sung PJ, Tai MH, Wen ZH, Chen NF, Kuo HM (2019) BA6 induces apoptosis via stimulation of reactive oxygen species and inhibition of oxidative phosphorylation in human lung cancer cells. Oxid Med Cell Longev 2019:6342104–6342104
10. Patricia M, de Groot CC, Wu, Brett W, Carter RFM (2018) The epidemiology of lung cancer. Transl Lung Cancer Res 1982:272-84
11. Elbendary AA, Hessain AM, El-Hariri MD, Seida AA, Moussa IM, Mubarak AS, Kabli SA, Hemeg HA, El Jakee JK (2018) Isolation of antimicrobial producing Actinobacteria from soil samples. Saudi J Biol Sci 25:44–46
12. Fang C, Gu L, Smerin D, Mao S, Xiong X (2017) The Interrelation between Reactive Oxygen Species and Autophagy in Neurological Disorders. Oxid Med Cell Longev 2017: 16
13. Ganesan P, Host R, David A, Daniel A, Rajiv M, Gabriel M, Ignacimuthu S, Al-dhabi NA (2017) Isolation and molecular characterization of actinomycetes with antimicrobial and mosquito larvicidal properties. Beni-Suef Univ J Basic Appl Sci 6:209–217
14. Hasan A, Haque E, Hameed R, Maier PN, Irfan S, Kamil M, Nazir A, Mir SS (2020) Hsp90 inhibitor gedunin causes apoptosis in A549 lung cancer cells by disrupting Hsp90:Beclin-1:Bcl-2 interaction and downregulating autophagy. Life Sci 256:118000
15. Iram S, Zahera M, Wahid I, Baker A, Raish M, Khan A, Ali N, Ahmad S, Khan MS (2019) Cisplatin bioconjugated enzymatic GNPs amplify the effect of cisplatin with acquiescence. Sci Rep 9:1–16
16. Lee LH, Azman AS, Zainal N, Eng SK, Ab Mutalib NS, Yin WF, Chan KG (2014) *Microbacterium mangrovi sp.* nov., an amylolytic actinobacterium isolated from mangrove forest soil. Int J Syst Evol Microbiol 64:3513–3519
17. Manivasagan P, Venkatesan J, Sivakumar K, Kim SK (2014) Pharmaceutically active secondary metabolites of marine actinobacteria. Microbiol Res 169:262–278
18. Musino D, Rivard C, Landrot G, Novales B, Capron I (2020) Tunable Ag Nanoparticle Properties in Cellulose Nanocrystals/ Ag Nanoparticle Hybrid Suspensions by H2O2 Redox Post-Treatment: The Role Of The H2O2/Ag Ratio. Nanomaterials 10:1559
19. Pfeffer CM, Singh ATK (2018) Apoptosis: A Target for Anticancer Therapy. Int J Mol Sci 19:448
20. Ravikumar S, Fredimoses M, Gnanadesigan M (2012) Anticancer property of sediment actinomycetes against MCF-7 and MDA-MB-231 cell lines. Asian Pac J Trop Biomed 2:92–96
21. Rivero-Montejo SD, Vargas-Hernandez M, Torres-Pacheco I (2021) Nanoparticles as Novel Elicitors to Improve Bioactive Compounds in Plants. Agriculture 11:134

22. Salim FM, Sharmili SA, Anbumalarmathi J, Umamaheswari K (2017) Isolation, molecular characterization and identification of antibiotic producing actinomycetes from soil samples. J Appl Pharm Sci 7:69–75
23. Saminathan K (2015) Biosynthesis of silver nanoparticles using soil Actinomycetes *Streptomyces* sp. Int J Curr Microbiol Appl Sci 4:1073–1083
24. Sanjivkumar M, Vaishnavi R, Neelakannan M, Kannan D, Silambarasan T, Immanuel G (2019) Investigation on characterization and biomedical properties of silver nanoparticles synthesized by an actinobacterium *Streptomyces olivaceus* (MSU3). Biocatal Agric Biotechnol 17:151–159
25. Santucci R, Sinibaldi F, Cozza P, Polticelli F, Fiorucci L (2019) Cytochrome c: An extreme multifunctional protein with a key role in cell fate. Int J Biol Macromol 136:1237–1246
26. Sharma P, Thakur D (2020) Antimicrobial biosynthetic potential and diversity of culturable soil actinobacteria from forest ecosystems of Northeast India. Sci Rep 10:1–18
27. Singh R, Dubey AK (2020) Isolation and characterization of a new endophytic actinobacterium *streptomyces californicus* strain adr1 as a promising source of anti-bacterial, anti-biofilm and antioxidant metabolites. Microorganisms 8:1–19
28. Singh V, Haque S, Singh H, Verma J, Vibha K (2016) Isolation, Screening, and Identification of Novel Isolates of Actinomycetes from India for Antimicrobial Applications. Front microbiol 7: 1921
29. Sivasankar P, Poongodi S, Seedevi P, Kalaimurugan D, Sivakumar M, Loganathan S (2019) Nanoparticles from Actinobacteria: A Potential Target to Antimicrobial Therapy. Curr Pharm Des 25:2626–2636
30. Vandamme M, Robert E, Lerondel S, Sarron V, Ries D, Dozias S, Sobilo J, Gosset D, Kieda C, Legrain B, Pouvesle J-M, Pape A Le (2012) ROS implication in a new antitumor strategy based on non-thermal plasma. Int J Cancer 130:2185–2194
31. WHO (2020) https://www.who.int/news-room/fact-sheets/detail/cancer. Accessed 26 Apr 2021
32. Zorov DB, Filburn CR, Klotz LO, Zweier JL, Sollott SJ (2000) Reactive oxygen species (ROS)-induced ROS release: A new phenomenon accompanying induction of the mitochondrial permeability transition in cardiac myocytes. J Exp Med 192:1001–1014
33. Zothanpuia AKP and BPS (2015) Molecular characterization of actinomycetes isolated from Tuichang river and their biosynthetic potential. Sci Vis 15:136–144

Tables

Table 1. Compounds present in Actinobacterial extract and their biological activities identified by GC-MS

Peak	Retention Time (min)	Area%	Name	Molecular Weight (g/mol)	Chemical formula	Similarity Index
Microbacterium proteolyticum LA2(R)						
1	14.149	25.10	n-Hexadecanoic acid	256	$C_{16}H_{32}O_2$	95
3	15.822	13.26	cis-Vaccenic acid	282	$C_{18}H_{34}O_2$	90
4	16.026	4.36	Octadecanoic acid	284	$C_{18}H_{36}O_2$	88
14	21.946	2.86	Cholesta-3,5-diene	368	$C_{27}H_{44}$	90
Streptomyces rochei LA2(O)						
1	14.175	36.88	n-Hexadecanoic acid	256	$C_{16}H_{32}O_2$	92
3	15.86	12.20	2-Hydroxycyclopentadecanone	240	$C_{15}H_{28}O_2$	83
12	21.947	5.77	carbonochloridate	448	$C_{28}H_{45}ClO_2$	81
16	23.776	13.49	Stigmast-5-en-3-o	678	$C_{47}H_{82}O_2$	84

Figures

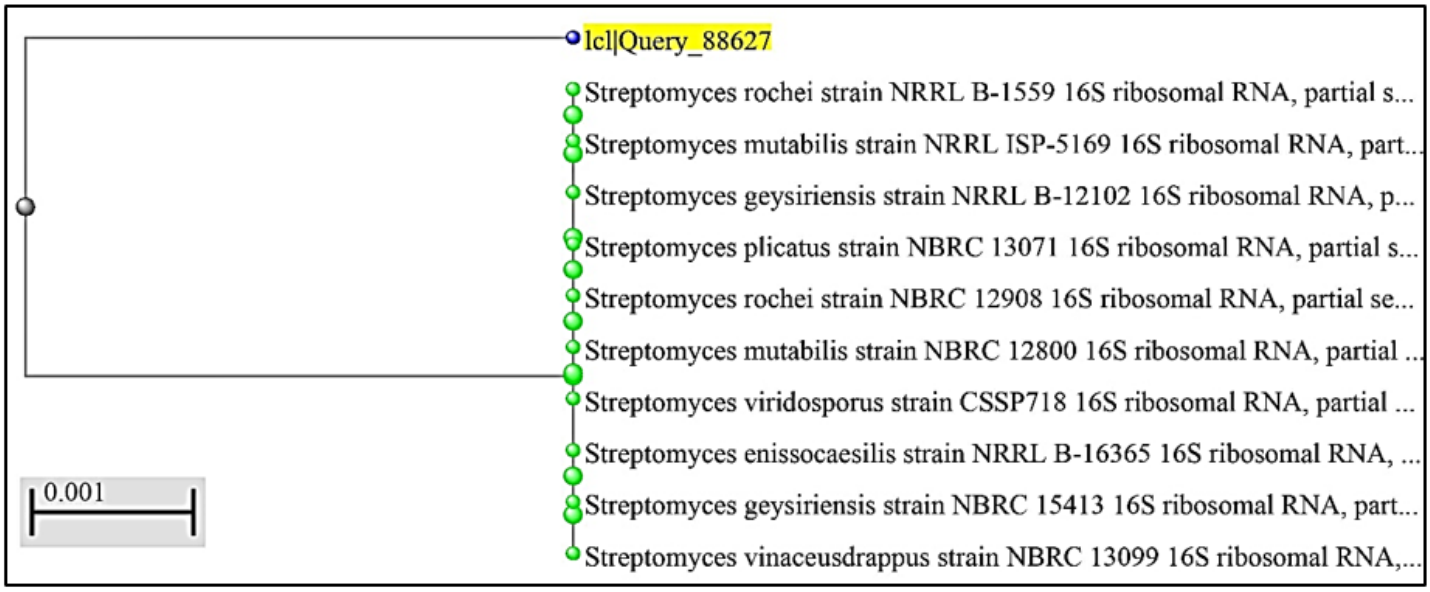

(a)

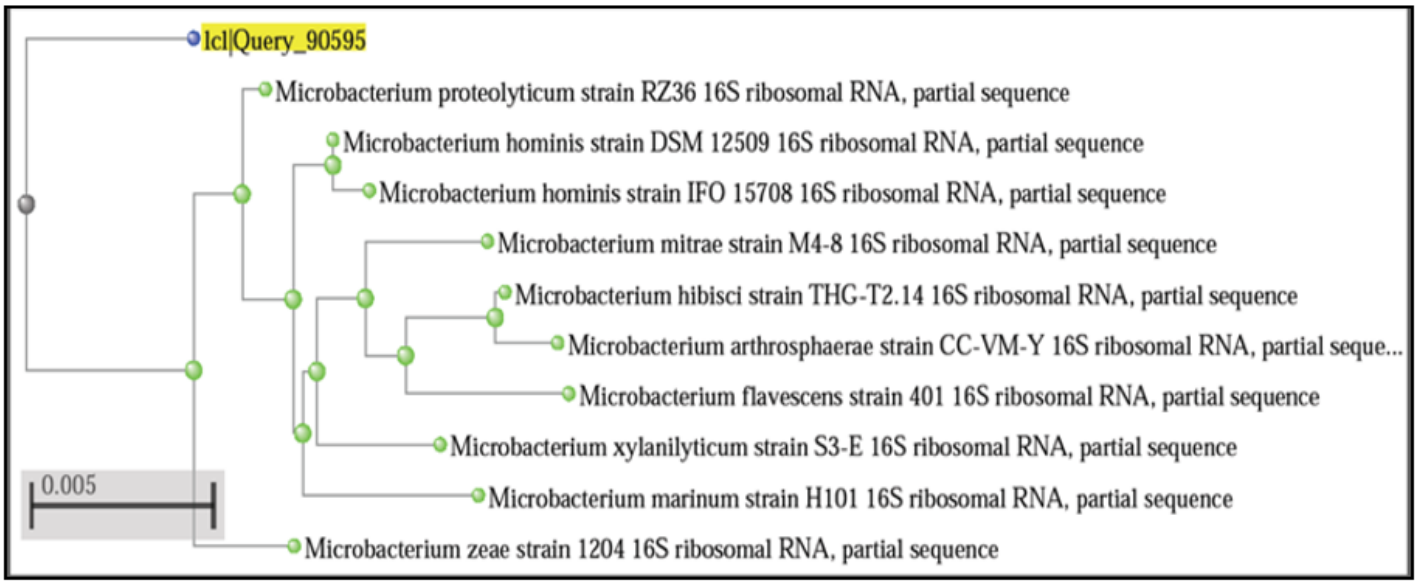

(b)

Figure 1

(a) Phylogenetic analysis of isolate LA2(O) (b) Phylogenetic analysis of isolate LA2(R)

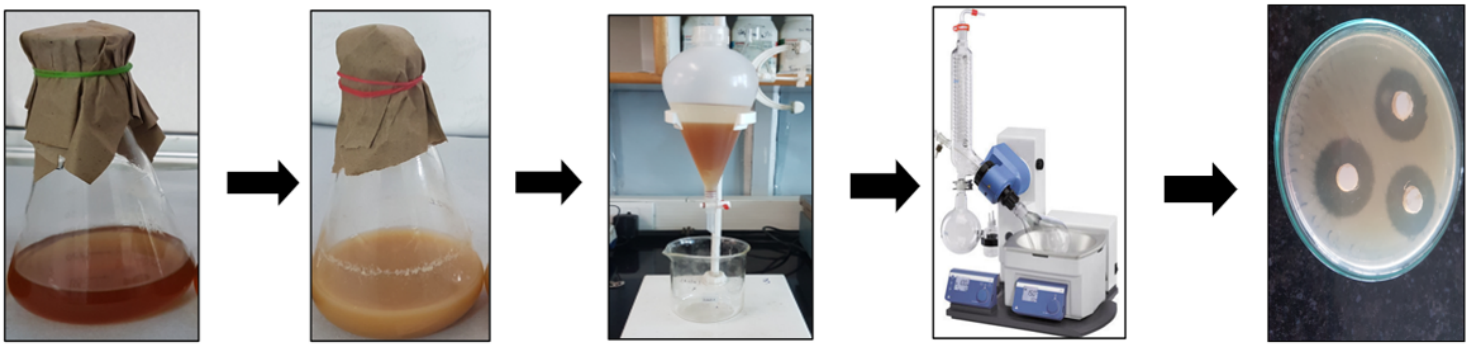

Figure 2

The procedure of secondary metabolite production and its antimicrobial activity

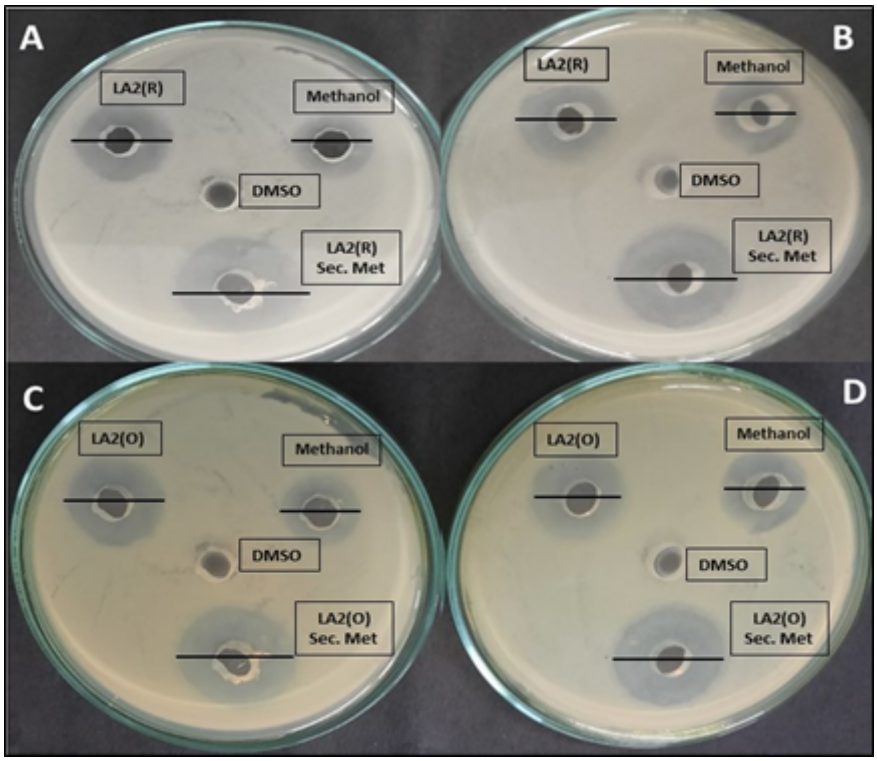

Figure 3

Antimicrobial activity of metabolites against pathogenic bacteria (A+B: antibacterial activity of S. aureus and C+D: antibacterial activity of K. pneumoniae)

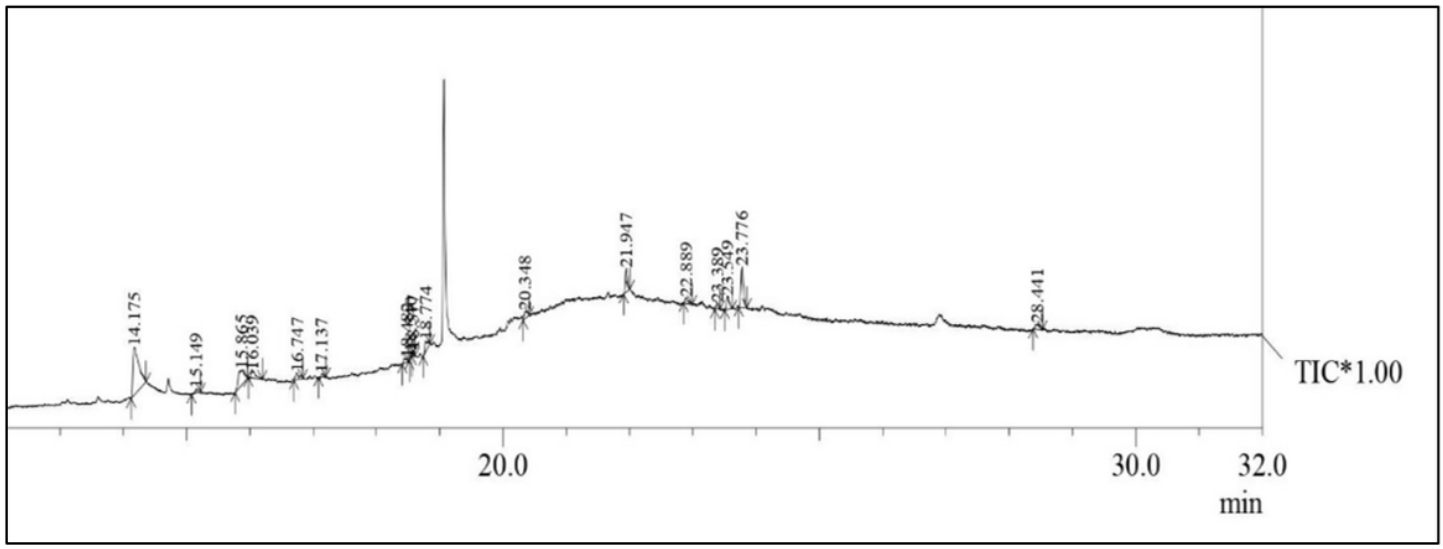

(a)

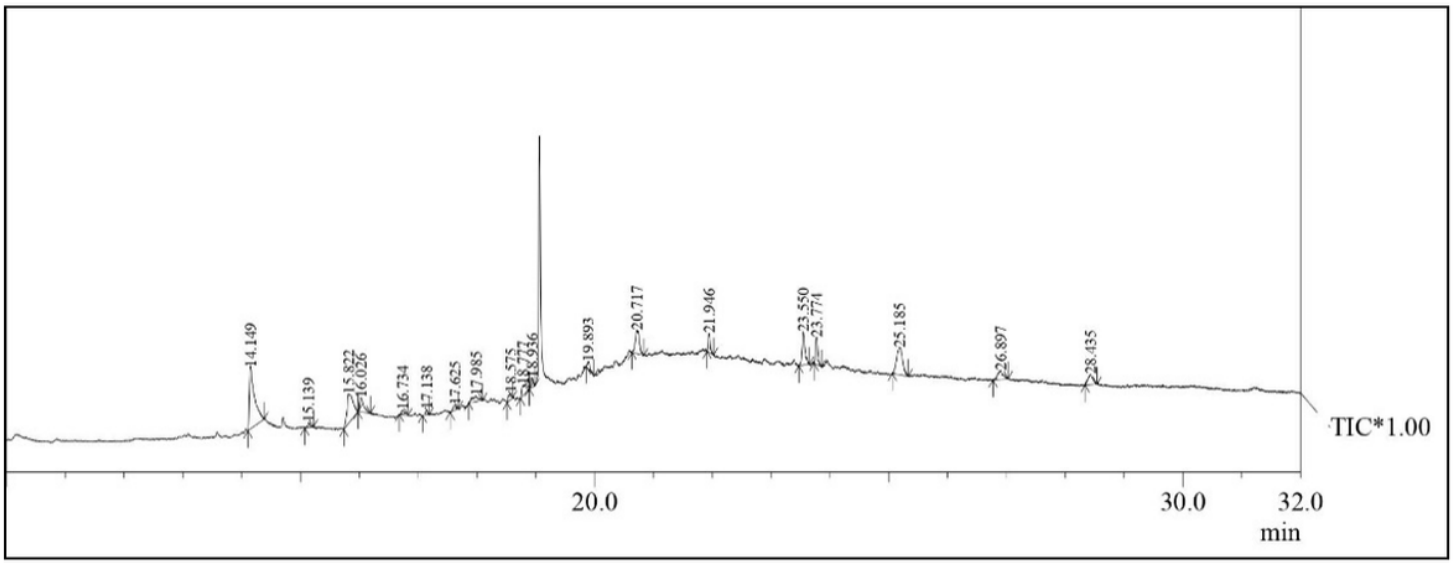

(b)

Figure 4

(a) GC-MS spectrum of secondary metabolite extracts prepared from Streptomycetes sp. LA2(O) (b) GC-MS spectrum of secondary metabolite extracts prepared from Microbacterium sp. LA2(R)

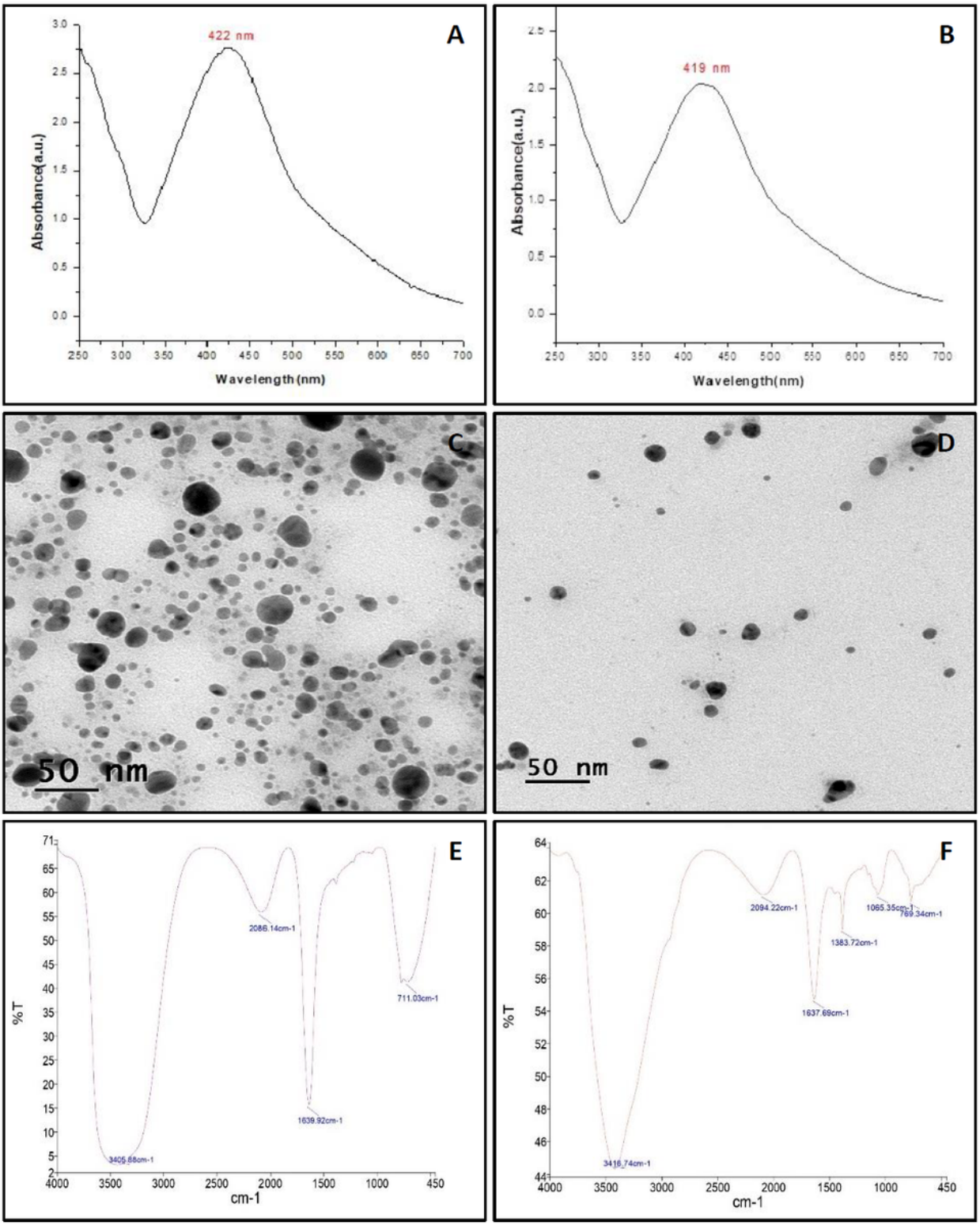

Figure 5

Characterization of Silver nanoparticles (A) LA2(R) and (B) LA2(O) under UV-Visible Spectroscopy. The AgNPs shows a distinct and fairly broad absorption peak centered at 422 and 419 nm, respectively. TEM micrograph of AgNPs from supernatant of (C)ON and (D)RN.

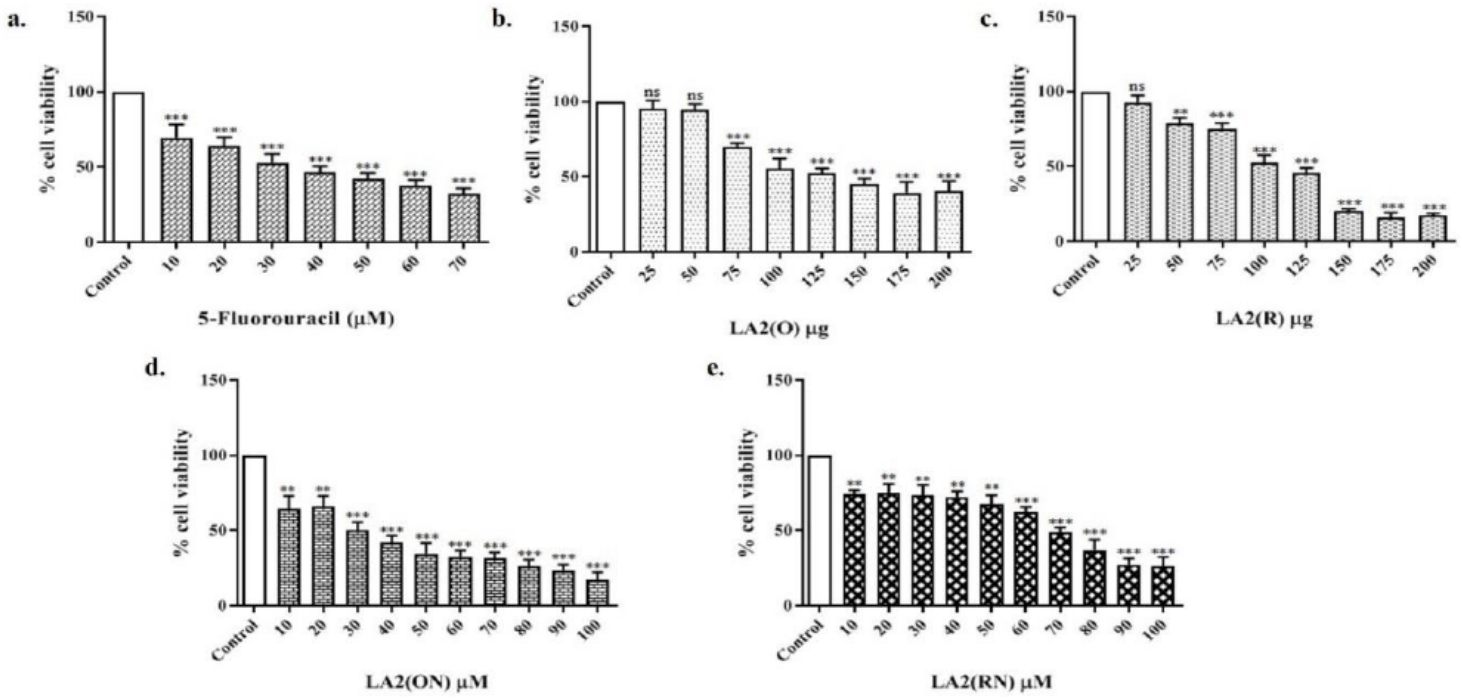

Figure 6

Effect of 5-Fluorouracil, secondary metabolites and their respective silver nanoparticles. MTT assay revealed that A549 lung cancer cells were inhibited in their proliferation. (a) 5-Fluorouracil, (b) LA2(O), (c) LA2(R), (d) LA2(ON) (e) LA2(RN) after 24h of treatment.

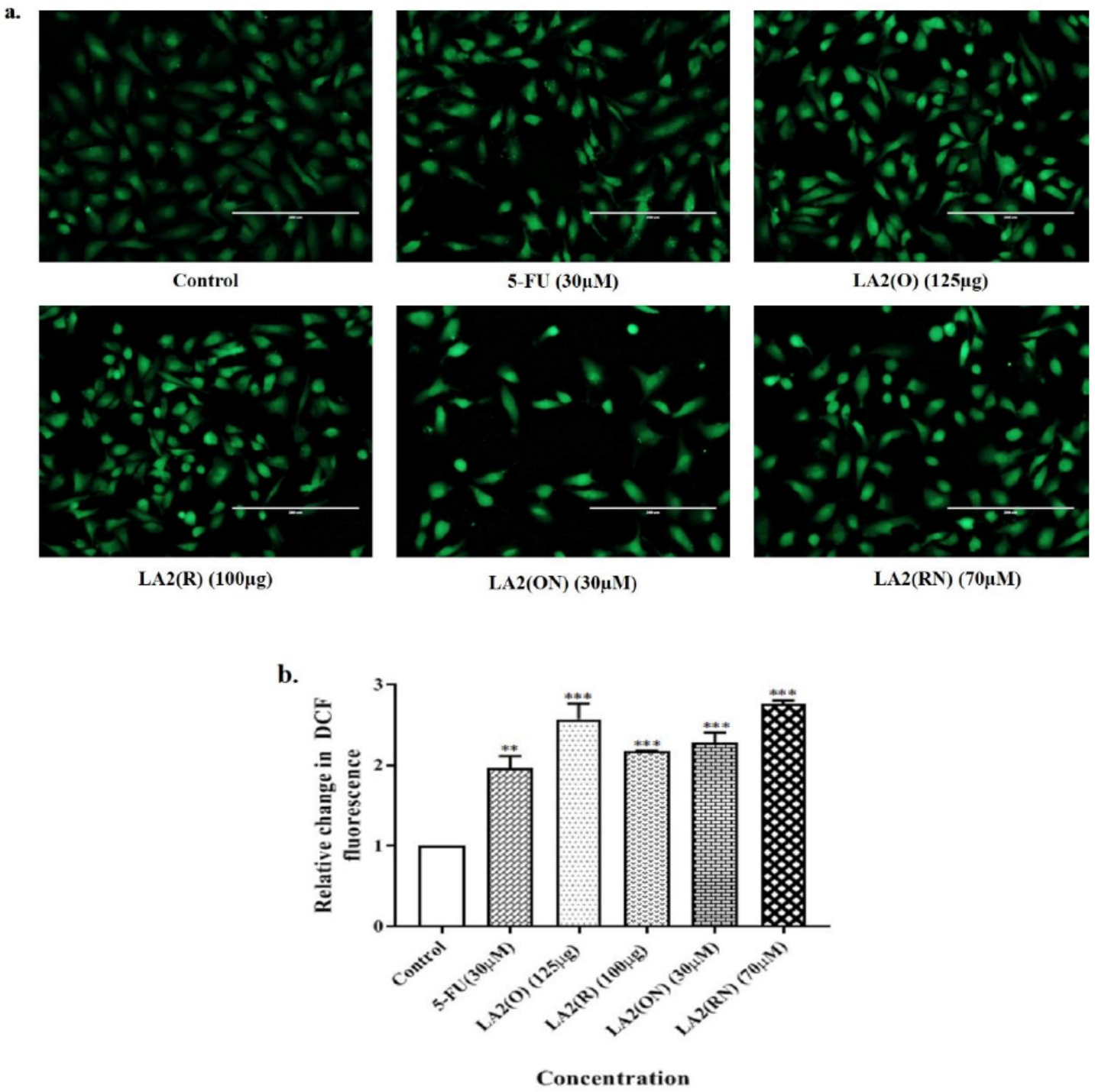

Figure 7

DCFDA staining was used to determine changes in ROS levels. (a) Fluorescence micrographs demonstrating ROS formation after 24 hours of treatment with the compounds. (b) Image J software was used to quantify the relative change in fluorescence intensity of DCFDA labelling in A549 cells on a graph.

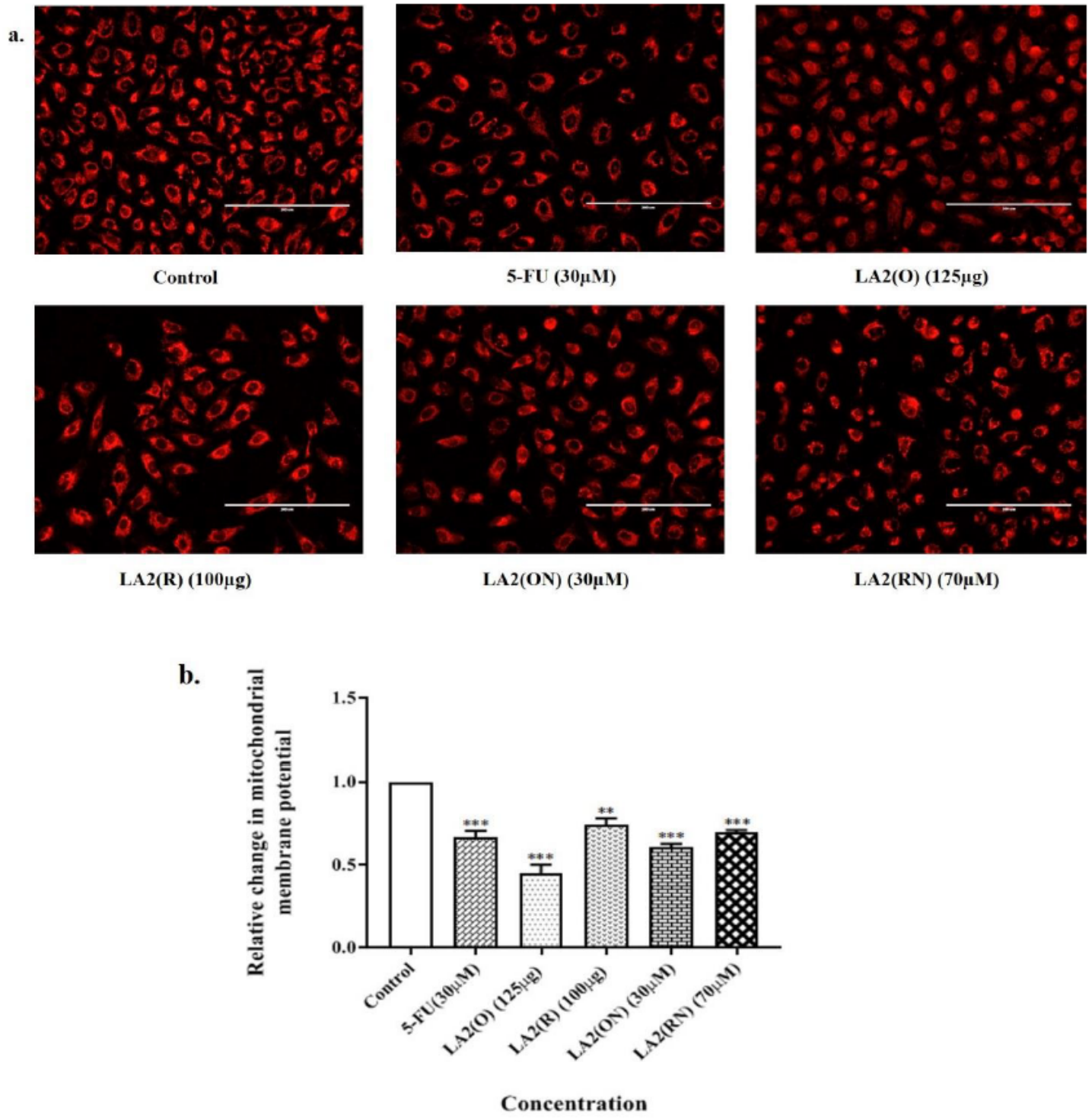

Figure 8

Mito Tracker Red staining was used to evaluate variations in the amount of mitochondrial membrane potential (MMP) in A549 cells. (A) MMP production fluorescence micrographs following treatment with the compounds for 24 hours (B) Image J software was used to quantify the relative change in fluorescence intensity of Mito Tracker Red staining in A549 cells on a graph. Scale Bar- 200µm. Key- 5-FU: 5-Fluorouracil.

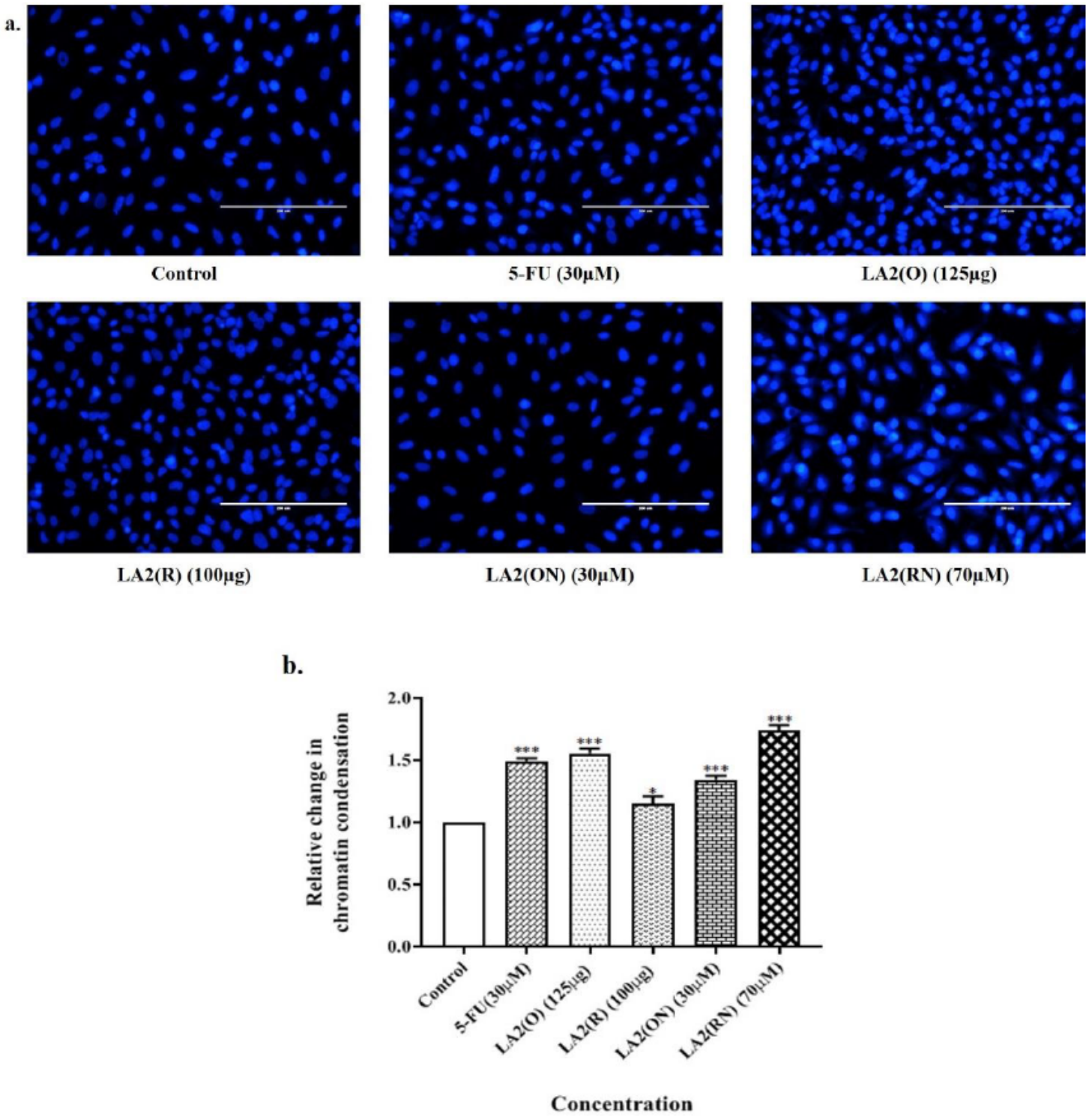

Figure 9

Consequence of the compounds on chromatin stability in lung cancer cells was explored by DAPI staining. (a) Fluorescence micrographs depict chromatin condensation after treatment with the compounds for 24h in A549 lung cancer cells. (b) Image J software was used to quantify the relative change in fluorescence intensity of DAPI staining in A549 cells on a graph. Scale Bar- 200µm. Key- 5-FU: 5-Fluorouracil.

Supplementary Files

This is a list of supplementary files associated with this preprint. Click to download.

- GraphicalAbstract.jpg
- CHECKLIST.docx